

Chemisorption of oxygen atoms on aluminum (100): A molecular-orbital cluster study

R. P. Messmer

General Electric Company, Corporate Research and Development, Schenectady, New York 12301

D. R. Salahub

Département de Chimie, Université de Montréal, Montréal, Canada H3C 3V1

(Received 14 July 1977)

Self-consistent-field $X\alpha$ scattered-wave molecular-orbital calculations have been performed for clusters of 5, 9, and 25 aluminum atoms representing the (100) surface in interaction with one, four, or five oxygen atoms at various positions above, in, and below the surface. Comparison of the results with recent ultraviolet and x-ray photoemission (UPS and XPS) results lend further support to the contention that at room temperature oxygen atoms are incorporated in or below the surface even at low exposure. Projected density of states curves for the 25-atom cluster with an oxygen atom centered in the first surface layer show three energy regions of significant oxygen character at about -9.5 , -7 , and -3 eV relative to the Fermi energy. Inspection of the wave functions for the corresponding levels shows that the -9.5 eV peak is due mainly to bonding combinations of in-plane oxygen p orbitals with aluminum s and p orbitals. The -7 -eV peak arises from both in-plane and out-of-plane oxygen p orbitals, again in bonding combinations while the orbitals responsible for the -3 -eV peak are best classified as nonbonding with respect to Al-O interactions. The two peaks at highest binding energy (-9.5 and -7 eV) have been observed in recent UPS experiments while at present there is only inconclusive evidence for the third and it is therefore suggested that a detailed angle and photon-energy dependent study be performed.

I. INTRODUCTION

In a previous paper¹ we presented results of a molecular-orbital study of aluminum clusters containing up to 43 atoms. In that study we examined the behavior of the calculated electronic structure as a function of the number of atoms in the cluster model and concluded that a cluster of 25 atoms in the C_{4v} symmetry appropriate to the (100) surface was sufficiently large to account in a satisfactory manner for the main features of the electronic structure of a clean aluminum surface. This cluster might therefore represent a reasonably converged model of an aluminum substrate for similar theoretical studies of the chemisorption of atoms and molecules on aluminum. In this paper we present results for the chemisorption of oxygen atoms on Al(100). Brief accounts of some of these results have already been published.²⁻⁴

In order to put our work in proper perspective we will begin with a concise review of experimental and previous theoretical work on the aluminum-plus-oxygen system. It will become apparent that although a number of different experiments have been performed on this system, certain key measurements remain to be made and we believe that our calculations will serve as useful guides in defining the parameters needed for further experiments.

Aluminum is a text-book example⁵ of a metal which on exposure to oxygen quickly forms a

protective oxide layer at the surface, thereby preventing further oxygen penetration and subsequent bulk oxidation. It is not this final aluminum-alumina system with which we are concerned here but rather the very earliest stages of oxidation, i.e., the chemisorption of oxygen atoms on a clean aluminum surface. We are concerned with the geometric structure and the electronic structure of the Al+O system, i.e., we seek answers to the questions: (i) Where are the oxygen atoms located? (ii) Where are the electrons of the system located, both in space and in energy?

As far as the first question is concerned the situation can be summarized rather succinctly. All available evidence for oxygen adsorption on polycrystalline Al films indicates that the oxygen atoms are incorporated in or slightly below the surface even at very low exposure. This conclusion stems from a large number of different techniques including kinetics studies involving the measurement of mass gain,⁶⁻⁸ measurements of changes in the work function,⁹ measurements of the angular dependence of plasmon peaks in the x-ray photoemission spectrum,¹⁰ (XPS) and secondary-ion-mass-spectroscopy (SIMS) measurements.¹¹ In addition, comparison of the positions of the oxygen-related features of ultraviolet and x-ray photoemission spectra,¹²⁻¹⁶ with theoretical results (see below) also favors oxygen incorporation. None of these methods are sufficiently powerful to yield the exact positions of the oxygen atoms. This information could possi-

bly be obtained, under favorable circumstances, from a detailed low-energy-electron diffraction (LEED) study of single-crystal faces.

Only recently have studies of oxygen chemisorption on single-crystal surfaces of Al have been performed. Gartland⁹ has carried out Auger-electron-spectroscopy (AES) and work-function measurements for the (100), (110), and (111) surfaces. He finds that the (100) and (111) surfaces behave quite differently from each other and proposes that the oxygen atoms adsorb randomly on Al(111) but form islands on Al(100). At the lowest level of oxygen exposure however, the work functions for both faces are nearly independent of oxygen coverage indicating that the net surface dipole is almost zero in both cases and therefore favoring a chemisorptive state with incorporated oxygen atoms. For the closely packed (111) surface this incorporation is likely accompanied by significant surface reconstruction while for (100) there is ample room in the fourfold sites for an oxygen atom to fit in with reasonable Al-O bond lengths. ($R_{\text{Al-O}} = 2.02 \text{ \AA}$ compared with $R_{\text{Al-O}} = 1.97 \text{ \AA}$ for the oxide Al_2O_3 .)

On the theoretical side the calculation of the equilibrium position of an oxygen atom in interaction with an aluminum surface presents enormous difficulties and has not yet been successfully done. The atom-jellium calculations of Lang and Williams¹⁷ predict an equilibrium position of 1.1 bohr above the jellium edge [which corresponds to 3.0 bohr above Al(100)] in disagreement with the experimental evidence. The reason for this failure is apparent on examination of the nature of the jellium substrate. If one moves an atom into the positive background the total energy rises much too quickly compared with the real situation of discrete nuclei. If one introduces the nuclei into the jellium model by using pseudopotentials¹³ this false repulsion is reduced in magnitude but still not enough to give an equilibrium geometry at or below the surface. The only other total energy calculations for this system are the self-consistent-field $X\alpha$ scattered-wave (SCF- $X\alpha$ -SW) calculations of Harris and Painter¹⁸ for the interaction of O with a five-atom aluminum cluster. Only positions at or beyond 2 bohr above the surface were considered. No minimum in the total energy was found and in any event the geometry predictions of this method in the muffin-tin approximation are known to be rather unreliable.¹⁹ (This does *not* mean that the one-electron wavefunctions are inaccurate. On the contrary spectroscopic^{20,21} and charge-density²² results indicate that they are very reliable. The difficulty in calculating the total energy arises from the fact that one uses a *charge density* of muffin-tin

form and this leads to inaccuracies which are much more serious than those caused by the muffin-tin form of the *potential* used to calculate the orbital wave functions and eigenvalues.)

It is unlikely that a reliable direct theoretical prediction of the oxygen positions will be forthcoming in the foreseeable future. However, indirect approaches may be useful. If one has experimental values for a given property and if this property can be reliably calculated for a number of oxygen positions then at least some information as to the likely geometry may be obtained (see below).

Once the positions of the oxygen atoms have been ascertained attention may be turned to the second question mentioned above, namely, that of the electronic structure. In fact this question cannot be rigorously separated from the previous one since the geometric and electronic structures are interdependent. The most direct means of obtaining information on the energy distribution of the electrons in a chemisorption system is by photoemission spectroscopy (UPS or XPS). Recently a number of UPS and XPS results have been reported for the aluminum plus oxygen system.¹²⁻¹⁶ Since these are the results with which we will compare our calculations we will give a rather detailed review of the experimental situation. We mention at this point that the complete picture is not yet at hand and that experimental studies are continuing. There is even at present some disagreement as to how many oxygen related features are present in the valence region.

UPS spectra for O on Al were reported in 1976 by two groups; Flodstrom *et al.*¹² and Yu *et al.*¹³ Both of these studies involved polycrystalline Al films. Flodstrom *et al.* used both He I (21.2-eV) and He II (40.8-eV) radiation. We reproduce in Fig. 1 their results using 40.8-eV photons for exposures of 1 and 5 L of O_2 (L = langmuir = 10^{-6} Torr sec). The reason we have chosen to show this spectrum rather than the He I results or the results of some of the other studies discussed below is that the spectra shown exhibit the maximum number of oxygen related features. Much recent work (e.g., Refs. 23-26) has shown that the photoemission results for surfaces and for chemisorption on surfaces can be extremely sensitive to the experimental parameters, namely, the angles of light incidence and electron emission, and the polarization and frequency of the exciting radiation. Therefore a single spectrum may not reveal all of the relevant features because of the dependence of intensity matrix elements on these parameters.

If one examines Fig. 1 and compares it with the spectrum for a clean aluminum film,¹⁴ three oxy-

gen related features may be distinguished. The two dominant features are a large peak centered at about 7 eV below the Fermi level (E_F) and a second peak which appears as a shoulder centered at -9.5 eV. The third feature is somewhat more questionable. If one compares the region between -5 eV and E_F for the case of 1 L exposure with the same region for a clean film then no new peaks are observed. Unfortunately, difference curves were not given. These would have been most useful to determine what, if any, is the difference at these energies between clean Al and Al exposed to 1 L of O_2 . If however one examines the spectrum for 5-L exposure one observes that the region between -5 eV and E_F has definitely changed, the valley at about -2 eV being filled in. Thus there is evidence for some oxygen related structure in this energy range although it should be stated at this point that other published spectra for different experimental parameters do not reveal this feature. In the work of Yu *et al.*,¹³ He I (21.2 eV) and a number of photon energies below 11.8 eV were used. Their reported He I spectrum shows only a single oxygen related peak at -7.2 eV. The spectra taken with lower-energy photons indicate an attenuation of the substrate emission between about -4 eV and E_F which also indicates that oxygen adsorption has some effect on the density of states in this energy range. There is no indication in the He I spectrum of the above-mentioned shoulder at -9.5 eV. The absence could possibly be explained if the experimental set up gave rise to particularly small differential cross sections for this region although a detailed calculation would be necessary to determine if

this is the case.

Further UPS results have been given by Flodström *et al.*¹⁴ Here the authors noted that the -7-eV peak changed position slightly (after a proper background subtraction) depending on whether He I or He II radiation was used. The values found were -7.1 and -6.8 eV, respectively. This is likely an effect of the frequency dependence of the matrix elements.

Very recently, Martinsson *et al.*¹⁶ have reported UPS results for oxygen on aluminum (100), (110), and (111) single-crystal surfaces. The spectra were taken with 21.2-eV photons and 25-L exposures of O_2 . For the (100) face the two peaks at -7 and -9.5 eV are clearly resolved. For (110) only one broad feature centered at about -7 eV is found while for (111) the -7-eV peak is present and is considerably narrower compared with the results for the other two faces. Thus it appears that the environment of the oxygen atoms is significantly different for these three surfaces of aluminum. In these three spectra there is no unambiguous evidence for prominent oxygen related structure in the region between -5 eV and E_F although the shape of the weak substrate signal is somewhat different for the three cases.

Another study of aluminum films by Flodström *et al.*¹⁵ used synchrotron radiation. Examination of the Al 2p core-level peaks provided evidence for a chemisorptive state with the Al 2p energy intermediate between that of clean Al and that of the aluminum oxide layer which is eventually formed. There was also a rather abrupt change in the valence region at an exposure of about 100 L indicating that the growth of an alumina layer starts at about this level of exposure. The results for the lower exposure cases (10-100 L) using 50-eV photons again show the -9.5- and -7-eV peaks. The region above -4 eV was not discussed.

One last photoemission work should be mentioned in order to bring this brief review as up to date as possible and that is the XPS work of Baird and Fadley¹⁰ who studied the angle dependence of core level (Al 2p and O 1s) plasmon satellite peaks. The authors conclude that for low exposure (10-15 L) the depth of oxygen penetration cannot be more than to 1-2 atomic layers. These results combined with the previously mentioned work function, kinetics, and SIMS data imply that the oxygen atoms are at or below the surface but do not dissolve in the bulk.

In summary, the available experimental information for oxygen chemisorption on polycrystalline aluminum and on single-crystal Al(100) shows two oxygen-related peaks at -9.5 and -7 eV. There is also some evidence for further oxygen related

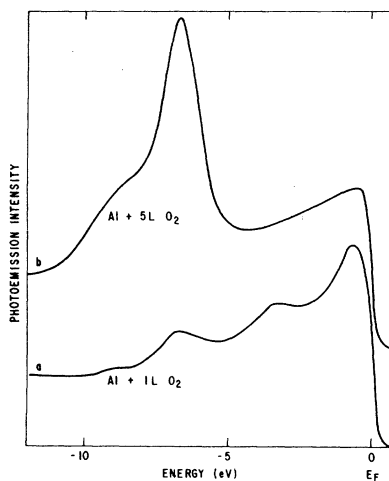


FIG. 1. Ultraviolet- ($h\nu = 40.8$ eV) photoemission spectra for oxygen chemisorbed on a polycrystalline aluminum film at 1- and 5-L exposures. Data are from Ref. 12.

structure near -3 eV although this is not definitive.

On the theoretical side with the exception of preliminary accounts of the present work²⁻⁴ there are only three published works which are relevant. The adatom-jellium calculations of Lang and Williams¹⁷ predicted a single oxygen $2p$ resonance at about -1.5 eV. The inclusion of the aluminum ion cores via pseudopotentials¹³ caused this resonance to broaden and go deeper into the band in somewhat better agreement with the experimental results, but still only one "resonance" was discussed. One must therefore conclude that this model is inadequate at least for a description of the polycrystalline and (100) faces where at least two oxygen related peaks have been observed. The only other theoretical study was by Harris and Painter.¹⁸ Here a five-atom cluster representing Al(100) in interaction with an oxygen atom was treated by the SCF- $X\alpha$ -SW molecular-orbital method. Only configurations with the oxygen 2 bohr or further above the surface were considered so that in light of the above evidence for oxygen incorporation it is not surprising that the results do not agree with the photoemission results. In addition we will show below that when the oxygen is in the surface the results for a five-atom cluster are significantly different from those for 9 or 25 atoms and so one must conclude that the small cluster is not an adequate model of the aluminum substrate for this case.

Hence there is a need for a theoretical treatment which is capable of accounting for the UPS data. We believe that the results presented below represent a significant step in this direction. As we shall see the peaks observed at -9.5 and -7 eV are accounted for in our calculations and their nature is elucidated. We also predict further oxygen related structure near -3 eV and believe that a more detailed experimental study of this region should be made.

In Sec. II we give the details of our calculations and in Sec. III we present our new results, emphasizing the behavior as a function of adsorbate-cluster distance and cluster size and comparing our results with experimental photoemission data.

II. MODELS, METHODS, AND PARAMETERS

The cluster models for the aluminum (100) surface which we consider here consist of 5, 9, and 25 atoms in C_{4v} symmetry. The coordinates of the atoms may be found in Ref. 1. In Fig. 2 we show the surface of the 25-atom cluster. This cluster consists of 12 atoms in the first surface plane, nine in the second, and four in the third. It thus contains all third neighbors of an adsor-

bate in the central fourfold site in the first surface layer. Calculations were performed for the five- and nine-atom clusters interacting with a single oxygen atom placed 4.0, 2.0, and 0.0 bohr above the surface plane ($Z_o = 4.0, 2.0, 0.0$). For the 25-atom cluster, only $Z_o = 2.0$ and 0.0 were considered for the case of a single adatom. In addition two further calculations were performed for this larger cluster. Five oxygen atoms were placed in the five available fourfold sites in the surface plane. This situation may be regarded as modeling the case of a monolayer oxygen coverage, although it must be emphasized that the five oxygens are not in equivalent environments; the outer ones lack certain aluminum neighbors which are present for the central oxygen. Finally four oxygen atoms were placed in the octahedral holes directly below the atoms labeled 1 in Fig. 2. This case therefore models the case of absorption in the second surface layer. Again in this configuration the oxygens have fewer aluminum next-nearest neighbors than for the central atom in the first layer and so we would expect the model to be less exact.

The calculations were performed with the SCF- $X\alpha$ -SW method which is described elsewhere.^{27,28} The muffin-tin (nonoverlapping sphere) approximation was used so that the sphere sizes were determined by the geometry. This was shown to be an adequate approximation for the aluminum substrate clusters in Ref. 1. Recent work^{19,29} has shown that in many instances for molecules better agreement with experimental ionization potentials and optical-transition energies can be obtained if one increases the sphere size and allows them to overlap. We have there-

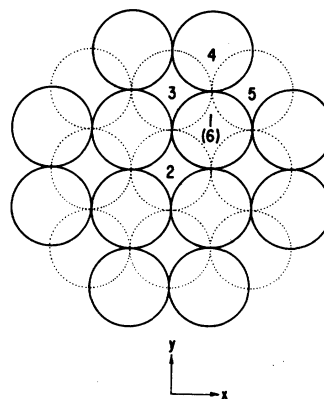


FIG. 2. View of the 25-atom cluster parallel to the (x, y) plane. The solid circles indicate atoms at $Z = 0.0$, the dotted circles, atoms at $Z = -3.821766$ bohr. There are four atoms (not shown) directly below Al(1) at $Z = -7.643530$ bohr. See Ref. 7 for coordinates.

fore also performed a calculation for $Al_{25} + O$ at $Z_0 = 0.0$ in which the oxygen sphere size was increased from its muffin-tin values of 1.12 to 1.56 bohr, an increase of 40%. As a point of comparison, the overlapping oxygen sphere radius for the CO molecule determined by Norman's³⁰ procedure is 1.4 bohr.¹⁹ The exchange parameters were taken from the compilation of Schwarz³¹ and have the value $\alpha = 0.72853$ for aluminum and $\alpha = 0.74447$ for oxygen. In the intersphere and extramolecular regions the aluminum value was used.

As usual the calculations were started by forming the potential from the superimposed potentials of neutral aluminum and neutral oxygen atoms and then iterating to self-consistency. The difference between the results for the zeroth iteration and the self-consistent results will therefore provide a measure of the importance of charge transfer in the system. This is discussed below.

In order to compare the calculated results with the results of photoemission experiments it is useful to generate density-of-states (DOS) curves of various types. The approximations involved and the explicit expressions used have been discussed elsewhere.¹ Three types of curves may be generated: (i) DOS—each molecular-orbital (MO) energy level is replaced by a Gaussian; (ii) difference in DOS (Δ DOS)—DOS curves are generated independently for the substrate and the substrate plus adsorbate system, the Fermi levels are aligned and then the substrate curve is subtracted point by point from the substrate plus adsorbate curve; (iii) projected or local DOS (PDOS or LDOS)—each Gaussian is weighted by the calculated orbital or total charge on a particular atomic center. For all of the curves presented below the Gaussian-width parameter has the value $\sigma = 0.05$ Ry.

If one then makes the necessary assumption (in the absence of further calculations) that effects due to intensity matrix elements, electron escape depths, and electronic relaxation may be neglected, then each of these types of DOS curves may be used in the interpretation of the photoemission results. Each type has certain advantages and disadvantages. The most straightforward to use are the DOS curves and these can be directly compared with experimental spectra if the above assumptions hold. For smaller clusters it is then rather easy to pick out new features due to the adsorbate. In the case of larger clusters; however, the DOS becomes dominated by the substrate contribution and it may be difficult to precisely determine the adsorbate features. In these cases it is then better to use Δ DOS or PDOS curves. The Δ DOS curves are analogous to the difference curves often generated by the experi-

mentalist. They give the change in the DOS on adsorption; however they do not reveal the source of the change, one does not know whether a particular feature of the Δ DOS curves is due primarily to adsorbate levels or, for instance, whether the feature is due to a more subtle interaction which changes the substrate contribution. This latter type of information is obtained from the PDOS curves which give directly the energy distribution for levels which have some adsorbate character. Clearly the latter two types of curves Δ DOS and PDOS are closely related since one would expect the largest changes in the DOS to occur at those energies for which the adsorbate makes a large contribution. Indeed for the $Al_{25} + O$ calculations discussed below either type of curve leads to the same conclusions as to the features to be expected in the photoemission spectrum. In what follows we will concentrate on PDOS curves; Δ DOS curves for some of the calculations may be found in Refs. 3 and 4 for comparison.

In the $X\alpha$ method, ionization potentials are calculated using Slater's transition-state method²⁷ in which half an electron is removed from the orbital of interest. This may produce relative shifts in the levels which must be taken into account for an accurate treatment. In general these shifts are smaller for delocalized orbitals than for localized ones. We have investigated these effects for a number of clusters. For $Al_5 + O$ at $Z_0 = 4.0$ bohr the calculated transition state shifts for all of the orbitals in the energy region of interest are 2.35 ± 0.15 eV while for $Al_5 + O$ at $Z_0 = 0.0$ the values are 2.56 ± 0.22 eV. Thus even for these relatively small clusters a uniform shift of all of the levels would give results of sufficient accuracy for our purposes. For the larger cluster, $Al_{25} + O$ at $Z_0 = 0.0$ we have calculated two transition state energies, the first for the orbital at -0.444 Ry which has a large fraction of the orbital change (12%) on the oxygen atom and the second for the orbital at -0.486 Ry which has zero charge on the oxygen. The calculated shifts were 1.44 and 1.41 eV, respectively. As expected these are smaller than for the more localized $Al_5 + O$ clusters. The latter results again indicate that sufficiently accurate results can be obtained by considering uniformly shifted orbital eigenvalues and this will be done for the remainder of the paper.

III. RESULTS AND DISCUSSION

We begin the discussion of our results by addressing two questions relevant to the choice of an adequate physical model and an adequate com-

putational method.

The first question has to do with the convergence of the results as a function of cluster size. This is a matter of prime importance if one wishes to simulate results for an infinite surface by a finite cluster. In our study of "clean" aluminum we saw that it is necessary to consider reasonably large clusters (25 atoms) in order to successfully interpret the photoemission results or in other words to obtain a good approximation to the DOS over the whole occupied bandwidth. Thus one may consider Al_{25} to be a "converged" model as far as "low-resolution" photoemission spectroscopy for the clean surface is concerned. One cannot however conclude from the above that it is necessary and sufficient to consider 25 Al atoms if one wishes to study chemisorption on Al(100). It is possible for either fewer substrate atoms to be adequate or for more substrate atoms to be required depending on the nature of the adsorbate-substrate interaction and on the energy resolution required for the experiment of interest (see Ref. 21 for a discussion). Of course the final test of whether a cluster model has converged rests on a comparison concerning its ability to satisfactorily account for the experimental data at the appropriate level of resolution.

In Fig. 3 we show PDOS curves for the oxygen atom at $Z_0=0.0$ (in the surface plane) for the Al_5 , Al_9 , and Al_{25} clusters. Only the occupied orbitals have been included in the generation of these curves. A cursory study of Fig. 3 is sufficient to conclude that for the case of oxygen incorporation only the 25-atom cluster has the possibility of

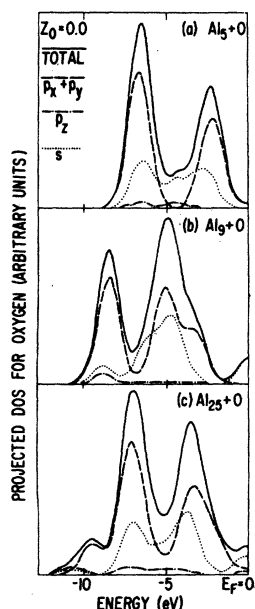


FIG. 3. Projected density of states for the oxygen atom vs orbital energy (eV relative to Fermi level E_F) for aluminum clusters interacting with an oxygen atom in the first surface plane ($Z_0=0.0$). (a) Al_5+O , (b) Al_9+O , (c) $Al_{25}+O$; solid lines, total PDOS; dashed lines, contribution from p_x and p_y orbitals; dotted lines, contribution from p_z orbitals; dashed-dot line, contribution from s orbitals.

providing a "converged" model. Both the Al_5 and Al_9 clusters would predict two oxygen-related peaks at this level of resolution, which is similar to the experimental resolution (see below). The $Al_{25}+O$ cluster however shows a third peak and is therefore qualitatively different from the two smaller clusters. As we pointed out in Ref. 4, this is not the case for large adsorbate cluster distances where all three clusters give quite similar results. Indeed for very large distances one also finds agreement with the results of the adatom-jellium model¹⁷ indicating that in the case of a weak interaction a rather approximate description of the substrate may be adequate. We will therefore not consider the five- and nine-atom clusters any further but rather restrict the discussion to the 25-atom cluster.

The second question we wish to discuss concerns the effects of self-consistency on the calculated results. Oxygen has an electronegativity, on the Pauling scale, of 3.50 while aluminum has a value of only 1.47. One would therefore expect an appreciable electron transfer from the aluminum atoms to the oxygen. In Fig. 4 we show the PDOS generated from the zeroth iteration for $Al_{25}+O$ ($Z_0=0.0$) i.e., the non-self-consistent result. These results are for the overlapping sphere calculation mentioned in Sec. II and may be compared with the corresponding self-consistent results given in Fig. 6. Clearly the effects of self-consistency are extremely important in this system. For the non-self-consistent case one finds the largest concentration of oxygen character at about -10 eV. As electronic charge flows from the aluminum to the oxygen this distribution spreads out in energy due to the formation of chemical bonds and the center of gravity of the distribution shifts to higher energy consistent with the increase of negative charge at the oxygen.

We will now examine the results for $Al_{25}+O$ in greater detail in order to provide an interpretation of the UPS results. In Table I we have gathered the calculated occupied orbital eigen-

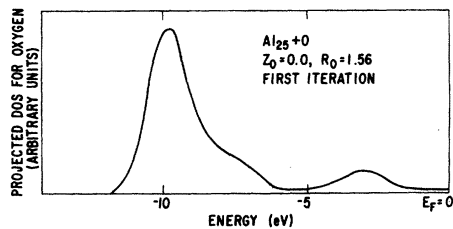


FIG. 4. Projected density of states for the oxygen atom for $Al_{25}+O$, $Z_0=0.0$ for a non-self-consistent calculation in which the potential is formed by superposing atomic potentials.

values and the calculated charges in the oxygen sphere for three different cases: (i) $Z_0 = 2.0$ bohr, (ii) $Z_0 = 0.0$ (muffin tin, $R_0 = 1.12$ bohr), and (iii) $Z_0 = 0.0$ (overlapping sphere $R_0 = 1.56$ bohr). Under C_{4v} symmetry the oxygen s and p_x orbitals transform as the a_1 irreducible representation and the oxygen p_x and p_y orbitals transform as e . Therefore only these representations will contribute to the PDOS curves. Figure 5 shows the PDOS curves for cases (i) and (ii). Each curve has been decomposed into contributions from s functions, p_x functions (a_1 levels), and $p_x + p_y$ functions (e levels) in order to characterize the features. When the oxygen is 2 bohr above the surface two peaks are present in the PDOS centered at about -2.5 and -5 eV. The available photoemission spectra show prominent features much deeper in the band at -7 and -9.5 eV and so if the model and the computational method are adequate one must conclude that the oxygen atoms are not at this position. If one moves the oxygen

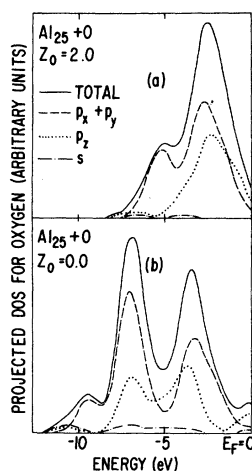


FIG. 5. Projected density of states for the oxygen atom for $Al_{25}+O$. (a) $Z_0 = 2.0$ bohr, (b) $Z_0 = 0.0$. Nonoverlapping spheres. See Fig. 3 for symbols.

into the surface in the central fourfold site then the curves in Fig. 5(b) result. Here we have peaks at about -9.5 , -7 , and -3 eV. As discussed at length above the first two peaks have been seen

TABLE I. Orbital eigenvalues ϵ (rydbergs) for the occupied valence levels of the $Al_{25}+O$ cluster. (i) $Z_0 = 2.0$ bohr, $R_0 = 1.61$ bohr; (ii) $Z_0 = 0.0$, $R_0 = 1.12$ bohr; (iii) $Z_0 = 0.0$, $R_0 = 1.56$ bohr. The numbers in parentheses give the separation in eV between the Fermi level and each level. Q_0 is the calculated fractional charge within the oxygen sphere for each level. The numbering of the levels includes only the valence molecular orbitals.

| Level | $Z_0 = 2.0$ | | | $Z_0 = 0.0, R_0 = 1.12$ | | | $Z_0 = 0.0, R_0 = 1.56$ | | | | |
|---------|-------------|---------|-------|-------------------------|-------------|---------|-------------------------|-------------|-------|---------|------|
| | $-\epsilon$ | | Q_0 | Level | $-\epsilon$ | Q_0 | Level | $-\epsilon$ | Q_0 | | |
| $1a_1$ | 1.738 | (17.65) | 0.81 | $1a_1$ | 1.918 | (19.92) | 0.58 | $1a_1$ | 2.071 | (22.71) | 0.76 |
| $2a_1$ | 1.203 | (10.37) | 0.01 | $2a_1$ | 1.229 | (10.68) | 0.04 | $2a_1$ | 1.188 | (10.69) | 0.07 |
| $1e$ | 1.088 | (8.80) | 0.00 | $1e$ | 1.138 | (9.43) | 0.05 | $1e$ | 1.130 | (9.90) | 0.24 |
| $3a_1$ | 1.001 | (7.62) | 0.01 | $3a_1$ | 1.031 | (7.99) | 0.01 | $2e$ | 0.997 | (8.09) | 0.24 |
| $1b_2$ | 0.970 | (7.20) | ... | $1b_2$ | 0.993 | (7.47) | ... | $3a_1$ | 0.996 | (8.08) | 0.25 |
| $1b_1$ | 0.946 | (6.87) | ... | $2e$ | 0.966 | (7.09) | 0.19 | $4a_1$ | 0.979 | (7.85) | 0.14 |
| $4a_1$ | 0.930 | (6.65) | 0.04 | $1b_1$ | 0.960 | (7.02) | ... | $1b_2$ | 0.956 | (7.54) | ... |
| $2e$ | 0.889 | (6.10) | 0.03 | $4a_1$ | 0.955 | (6.94) | 0.18 | $1b_1$ | 0.927 | (7.14) | ... |
| $3e$ | 0.838 | (5.40) | 0.04 | $3e$ | 0.892 | (6.10) | 0.03 | $3e$ | 0.863 | (6.27) | 0.01 |
| $4e$ | 0.808 | (4.99) | 0.10 | $4e$ | 0.837 | (5.35) | 0.01 | $4e$ | 0.811 | (5.56) | 0.01 |
| $5a_1$ | 0.755 | (4.27) | 0.01 | $5a_1$ | 0.825 | (5.17) | 0.09 | $5a_1$ | 0.791 | (5.29) | 0.09 |
| $2b_2$ | 0.749 | (4.19) | ... | $2b_2$ | 0.777 | (4.53) | ... | $2b_2$ | 0.736 | (4.54) | ... |
| $2b_1$ | 0.736 | (4.01) | ... | $2b_1$ | 0.744 | (4.08) | ... | $2b_1$ | 0.719 | (4.31) | ... |
| $6a_1$ | 0.723 | (3.84) | 0.11 | $6a_1$ | 0.731 | (3.90) | 0.04 | $6a_1$ | 0.716 | (4.27) | 0.07 |
| $1a_2$ | 0.694 | (3.44) | ... | $7a_1$ | 0.712 | (3.64) | 0.15 | $1a_2$ | 0.679 | (3.77) | ... |
| $5e$ | 0.689 | (3.37) | 0.05 | $1a_2$ | 0.702 | (3.51) | ... | $5e$ | 0.676 | (3.73) | 0.07 |
| $7a_1$ | 0.677 | (3.21) | 0.00 | $5e$ | 0.699 | (3.47) | 0.08 | $7a_1$ | 0.674 | (3.70) | 0.04 |
| $6e$ | 0.654 | (2.90) | 0.15 | $6e$ | 0.695 | (3.49) | 0.04 | $6e$ | 0.665 | (3.58) | 0.01 |
| $3b_2$ | 0.640 | (2.71) | ... | $8a_1$ | 0.693 | (3.39) | 0.02 | $8a_1$ | 0.661 | (3.52) | 0.01 |
| $8a_1$ | 0.614 | (2.35) | 0.33 | $3b_2$ | 0.669 | (3.06) | ... | $3b_2$ | 0.628 | (3.07) | ... |
| $7e$ | 0.594 | (2.08) | 0.11 | $7e$ | 0.601 | (2.14) | 0.06 | $7e$ | 0.576 | (2.37) | 0.05 |
| $4b_2$ | 0.570 | (1.76) | ... | $3b_1$ | 0.584 | (1.90) | ... | $4b_2$ | 0.557 | (2.11) | ... |
| $3b_1$ | 0.556 | (1.56) | ... | $4b_2$ | 0.584 | (1.90) | ... | $3b_1$ | 0.540 | (1.88) | ... |
| $8e$ | 0.523 | (1.12) | 0.06 | $8e$ | 0.582 | (1.88) | 0.00 | $8e$ | 0.535 | (1.81) | 0.00 |
| $9a_1$ | 0.512 | (0.97) | 0.18 | $9a_1$ | 0.516 | (0.98) | 0.01 | $9e$ | 0.485 | (1.13) | 0.00 |
| $9e$ | 0.499 | (0.79) | 0.00 | $9e$ | 0.513 | (0.94) | 0.00 | $9a_1$ | 0.484 | (1.12) | 0.01 |
| $10a_1$ | 0.491 | (0.68) | 0.01 | $4b_1$ | 0.486 | (0.57) | ... | $2a_2$ | 0.453 | (0.69) | ... |
| $4b_1$ | 0.470 | (0.39) | ... | $2a_2$ | 0.477 | (0.45) | ... | $4b_1$ | 0.453 | (0.69) | ... |
| $2a_2$ | 0.469 | (0.38) | ... | $5b_2$ | 0.467 | (0.31) | ... | $5b_2$ | 0.429 | (0.37) | ... |
| $5b_2$ | 0.443 | (0.03) | ... | $10e$ | 0.453 | (0.12) | 0.01 | $10e$ | 0.415 | (0.18) | 0.00 |
| $10e$ | 0.441 | (0.00) | 0.00 | $10a_1$ | 0.444 | (0.00) | 0.13 | $10a_1$ | 0.402 | (0.00) | 0.08 |

in UPS studies while there is some (inconclusive) evidence for the third. Before discussing the comparison with experiment further we wish to examine the sensitivity of our results to some of the more important parameters of the model and of the method. Basically we seek answers to the following three questions: (i) What happens to the above three peaks if one uses a larger oxygen sphere? (ii) What happens to them if one allows more oxygen atoms to adsorb at the surface four-fold, $Z_0 = 0.0$, sites? (iii) What happens to them if one puts the oxygen atoms further below the surface, i.e., if one surrounds them entirely by aluminum atoms. We will examine each of these questions in turn. In Fig. 6 we present the PDOS for oxygen for the case of overlapping spheres. Comparison of this figure with Fig. 5(b) reveals that the three peaks mentioned above are still present at approximately the same energies. Moreover the decomposition of each peak into in-plane ($p_x + p_y$) and out-of-plane (p_z) components is quite similar in both cases. The -9.5 -eV peak is almost entirely due to in-plane orbitals while the other two peaks receive significant contributions from both types of orbitals. The main difference between the two figures is in the relative intensities of the peaks. In the overlapping sphere case the -9.5 -eV peak is stronger and the -3 -eV peak weaker with respect to their relative intensities in the muffin-tin case. We therefore conclude that while the finer details of the binding and electronic structure depend to some extent on the oxygen sphere size, a result to be expected from previous molecular studies, as far as the existence of the three regions of high oxygen character is concerned both calculations give the same qualitative (and semiquantitative as far as the energies are concerned) results.

In order to provide an answer to the second question posed above we have carried out calculations for the case of five oxygen atoms in the

five fourfold sites of the first surface layer. Since the central hole site has an environment closer to that for an infinite surface we concentrate on the PDOS for the oxygen at this site. The other four oxygens lack a number of second-neighbor aluminum atoms and so this cluster should represent a less well-converged model for these atoms. The PDOS curve for this atom is shown in Fig. 7. Comparison of this curve with Fig. 5(b) again shows that the three peaks discussed above are present but with somewhat altered intensities. The decomposition of the peaks into in-plane and out-of-plane components is again quite similar, except for one difference, which may turn out to be detectable by angle resolved photoemission studies. For the case of a single oxygen atom the in-plane and out-of-plane components of the -7 - and the -3 -eV peaks have their maxima at almost the same energies. When one adds nearby oxygen atoms these shift somewhat and for the case of $Al_{25} + 5 O$ are separated by 1 eV or so. It is expected that the two types of orbitals will have somewhat different angular dependences in photoemission (see below). Moreover, if the experimental inference mentioned above is correct and oxygen tends to chemisorb on Al(100) in islands rather than randomly, then the $Al_{25} + 5 O$ cluster might prove to be a good model even at rather low exposures. Under these circumstances it is therefore possible that a detailed angle-resolved photoemission experiment could reveal up to five different "oxygen peaks" at the resolution so far obtained for this system.

The third question posed above; namely, what happens to these peaks when the oxygen atoms are pushed deeper below the surface, can only be answered somewhat more approximately than the preceding two questions. We have done a calculation for the case of four oxygen atoms placed in the octahedral interstices immediately below the aluminum atoms labeled 1 in Fig. 2 ($Z_0 = -3.82$

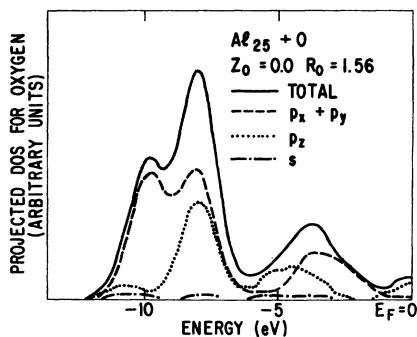


FIG. 6. Projected density of states for the oxygen atom for $Al_{25} + O$, $Z_0 = 0.0$. Overlapping Al and O spheres. ($R_0 = 1.56$ bohr). See Fig. 3 for symbols.

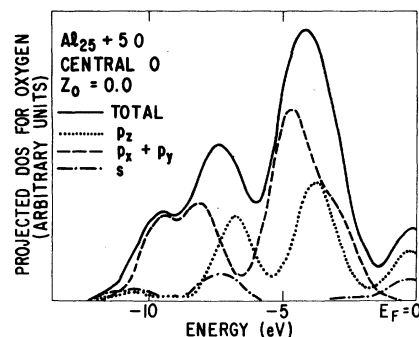


FIG. 7. Projected density of states for the central oxygen atom for $Al_{25} + 5 O$, $Z_0 = 0.0$. See Fig. 3 for symbols.

bohr). In this position the oxygens are in contact with aluminum atoms which are missing a number of the neighbors which they would have in the case of the semi-infinite solid and hence the results should be somewhat less reliable than for the cases discussed above. Nevertheless, we present in Fig. 8 the PDOS for these oxygen atoms in order to demonstrate the degree of sensitivity of the results to the details of the oxygen atom environment. Figure 8 has certain points of similarity and also certain differences when compared with Fig. 5(b). (Here the oxygens are not on the four-fold axis and so a decomposition into p_x and $p_x + p_y$ components has not been made). The lowest binding-energy peak has moved down somewhat to about -4 eV and there is now a rather broad oxygen related region which extends from about -7 to beyond -10 eV and a definite shoulder at about -12 eV. Thus we see that the PDOS curves are rather sensitive to the environment of the oxygen atom.

In summary, the above results indicate oxygen related features at about -9.5 , -7 , and -3 eV for the case of oxygen incorporation in the first surface layer. These three features are present but with differing relative magnitude whether one considers the adsorption of a single oxygen atom, or five neighboring atoms, and whether one uses the nonoverlapping sphere approximation or allows the aluminum spheres and the oxygen sphere to overlap. We will now discuss the nature of the molecular orbitals which give rise to these features in order to better characterize the aluminum-oxygen binding. In order to do this we have generated contour maps of the orbital wave functions for all orbitals which have more than 5% of their charge within the oxygen sphere. These are shown in Fig. 9 for the a_1 orbitals, i.e., those involving oxygen p_x orbitals and in Fig. 10 for the e orbitals, i.e., those involving oxygen p_x and p_y orbitals. We begin the discussion of these plots with a general com-

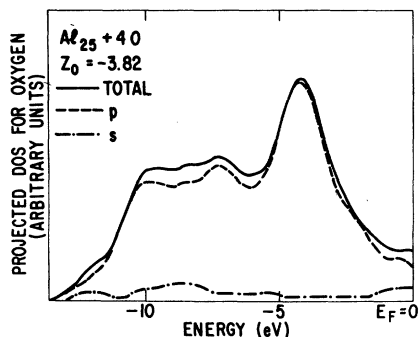


FIG. 8. Projected density of states for the oxygen atom for $Al_{25} + 4 O$, $Z_0 = 3.82$ bohr. Dashed line, p contribution; dash-dot line, s contribution.

ment. In all of the cases shown the region around the oxygen atom contained a large number of very closely spaced contours, which would be unresolved on the figures. These areas are represented on the figures by the black regions for positive values of the wave functions and by the hatched regions for negative values. Thus the electron density is very large in this region and the gradient is also large, the density falling off rapidly as one moves away from the nucleus. The aluminum contours on the other hand represent a much more diffuse electron distribution.

The contour plots in Figs. 9 and 10 may be classified into three types as far as the aluminum-oxygen interactions are concerned; bonding, nonbonding, and antibonding. For the a_1 symmetry there is only one bonding orbital, Fig. 9(d), and this occurs at -6.94 eV. Figures 9(b) and 9(c) represent nonbonding- and antibonding-type interactions. Finally the orbital in Fig. 9(a) which is the highest occupied orbital of the cluster is best classified as antibonding.

For the in-plane orbitals, e symmetry, there are two bonding orbitals Figs. 10(c) and 10(d) which have energies of -7.09 and -9.43 eV, respectively. The remaining two orbitals, Figs. 10(a) and 10(b), show very little interaction between the oxygen functions and the aluminum functions and are therefore nonbonding. Hence the principal character of the three main peaks

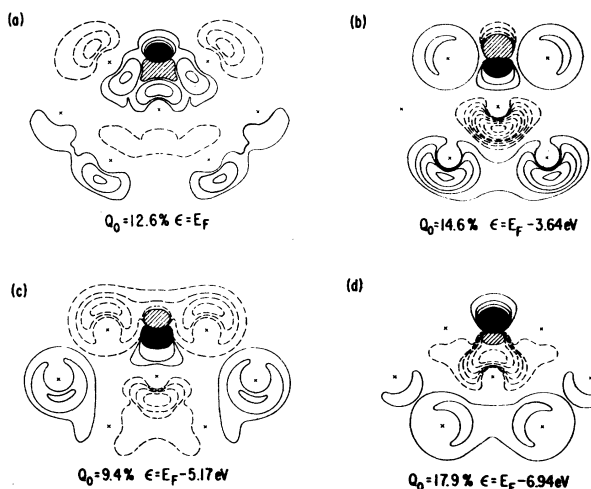


FIG. 9. Contour maps of selected a_1 molecular orbital wave functions for $Al_{25} + O$, $Z_0 = 0.0$. The plots are in a plane parallel to the z axis and at 45° to the x axis. (See Fig. 2.) The solid (positive) and hatched (negative) regions near the oxygen atom represent regions of many closely spaced contours. Solid lines, positive value of wave function. Dashed lines, negative value of wave function. The levels shown are at (a) 0.0, (b) -3.64 , (c) -5.17 , and (d) -6.95 eV with respect to the Fermi level.

found in the oxygen PDOS is as follows. The peak at -9.5 eV is primarily due to a bonding e type orbital. That at -7 eV receives important contributions from bonding orbitals of both a_1 and e types and that at -3 eV is due to nonbonding orbitals, again of both symmetry types.

It is interesting that a recent SCF- $X\alpha$ -SW study^{32,33} of the AlO_4^{5-} and AlO_6^{9-} clusters chosen to represent aluminum oxide also finds three distinct energy regions of high oxygen content. For the AlO_4^{5-} cluster bonding MO's are found at about -5.5 and -2.5 eV (with respect to the Fermi level) and three nonbonding levels are found between -2 eV and E_F . It is also noteworthy that in the photoemission spectrum of oxygen adsorbed on polycrystalline films of copper,³⁴ three oxygen-related regions are found at -2 , -7.5 (with a shoulder at -9), and -13 eV. The above have been cited merely as examples where simple ideas of chemisorption such as the formation of distinct orbital resonances with single well defined adsorbate orbital parentage are not always applicable.

The principal outstanding question about the $Al(100)$ +oxygen system at low exposure concerns the existence of the feature at -3 eV. Our calculations predict its existence. The present experimental evidence is at best inconclusive. We believe the solution of this problem lies in the

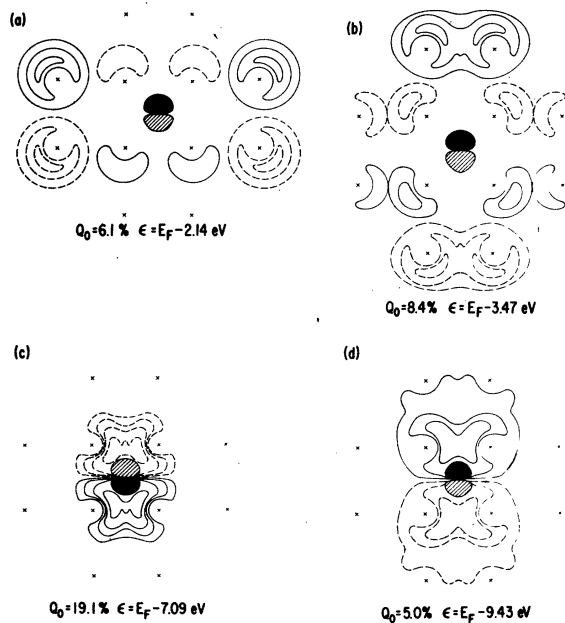


FIG. 10. Contour maps of selected molecular-orbital wave functions for $Al_{25} + O$, $Z_0 = 0.0$. The plots are in the xy plane (see Fig. 2). See Fig. 9 for symbols. The levels shown are at (a) -2.14 , (b) -3.47 , (c) -7.09 , and (d) -9.43 eV with respect to the Fermi level.

detailed angular and photon-energy dependence of the photoemission process. There is now ample experimental evidence²³⁻²⁵ for the great sensitivity of the photoemission cross section to the angle of light incidence, the polarization of the incident photons, and the exit angles at which the emitted electrons are collected. It is now possible, following the work of Davenport²⁶ to calculate photoemission intensities within the framework of the SCF- $X\alpha$ -SW method and such calculations are now being prepared for the aluminum plus oxygen clusters and when they are completed should be of help in choosing the most favorable experimental parameters in order to find the -3 -eV structure if it exists.

In order to illustrate the large changes which can result if one varies the photon energy and the angles we have used Davenport's method to calculate the intensities to be expected for the AlO molecule for a number of experimental configurations. These results are *not* intended to be relevant to the oxygen chemisorption case; clearly this would be an inadequate model. They are merely intended to be illustrative of the possible large effects of the experimental parameters on the observed photoemission spectrum. The parameters which are at the disposal of the experimentalist are shown in Fig. 11 while in Fig. 12 we show the differential cross sections calculated for the 5σ , 6σ , and 2π orbitals of an AlO molecule oriented along the z axis, as a function of the electron exit angle for two different photon energies (21.2 and 50.0 eV). The only point which we wish to make from these figures is that the emission due to a given orbital can vary by an order of magnitude depending on the experimental setup.

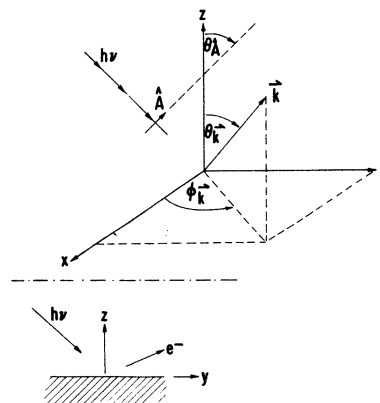


FIG. 11. Experimental parameters which may be varied in an angular-resolved photoemission experiment: $h\nu$, frequency of exciting radiation; θ_A , polar angle for electric vector of exciting radiation (assumed in the yz plane); θ_k , ϕ_k , polar and azimuthal angles for detector.

We believe that our calculations are sufficiently accurate that the presence or absence of a gross feature such as the oxygen related feature at -3 eV should not be falsely predicted and we therefore believe that a detailed experimental search in this energy region is called for.

The final point which we wish to discuss concerns the position of the aluminum $2p$ core levels in the presence of oxygen. Flodström *et al.*¹⁵ have measured photoemission spectra in this energy region using synchrotron radiation. For polycrystalline films they find that at low oxygen exposure a new peak develops at about a 1.3-eV higher binding energy than for the case of clean aluminum. At higher exposures yet another peak grows in at about 2.6 eV with respect to the clean aluminum value, which is very near to the value observed for aluminum oxide. These results are interpreted in terms of a two-stage oxidation. The 1.3-eV peak corresponds to a "chemisorptive" state while the 2.6-eV peak corresponds to the formation of an aluminum oxide layer. Very recently³⁵ similar studies have been performed for single-crystal Al(111) and Al(100). The Al(111) results are very similar to those for the films discussed above while for the (100) face the intermediate peak was not observed for the lowest exposure considered (50 L). These results are

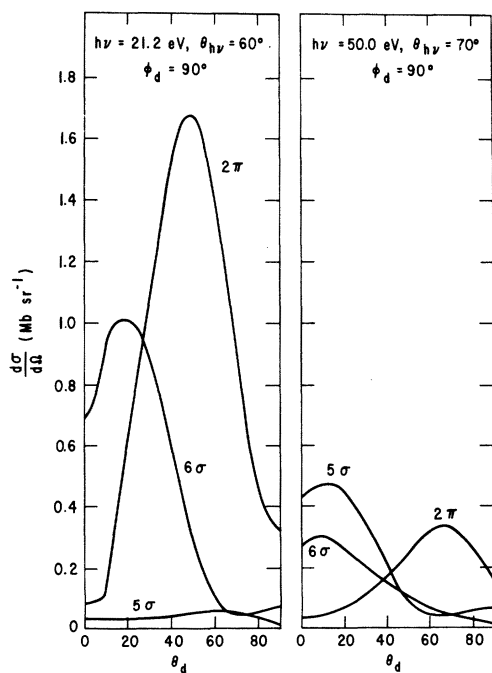


FIG. 12. Differential cross sections ($d\sigma/d\Omega$) (Mb sr^{-1}) vs polar angle of detector θ_d for the 2π , 5σ , and 6σ orbitals of an AlO molecule oriented along the z axis calculated by Davenport's method (Ref. 26) for unpolarized light of energy (a) 21.2 eV, (b) 50 eV.

TABLE II. Orbital eigenvalues ϵ_{2p} (rydbergs) for the Al $2p$ derived levels of the Al_{25} and $\text{Al}_{25} + \text{O}$ clusters. The numbers in parentheses are the shifts in eV with respect to the corresponding value for Al_{25} . See Fig. 2 for numbering convention.

| | Al_{25} | | $Z_0 = 2.0$ | | $Z_0 = 0.0$ | |
|--------|------------------|-----------------|-------------|-----------------|-------------|--|
| | ϵ_{2p} | ϵ_{2p} | Δ | ϵ_{2p} | Δ | |
| Al (1) | -5.365 | -5.431 | (0.65) | -5.442 | (1.05) | |
| Al (2) | -5.370 | -5.392 | (0.30) | -5.459 | (1.21) | |
| Al (3) | -5.362 | -5.373 | (0.15) | -5.376 | (0.19) | |
| Al (4) | -5.387 | -5.411 | (0.33) | -5.423 | (0.49) | |
| Al (5) | -5.374 | -5.411 | (0.50) | -5.430 | (0.76) | |
| Al (6) | -5.381 | -5.387 | (0.08) | -5.411 | (0.41) | |

consistent with the conclusion of Gartland⁹ mentioned above that adsorption occurs randomly on Al(111) but that oxide islands form on Al(100). Thus the 1.3-eV peak can most likely be attributed to aluminum atoms which have only one nearby oxygen atom while the 2.6-eV peak corresponds to aluminum atoms surrounded by several oxygens. In this respect it would be interesting to have experimental results for Al(100) at low temperatures and the lowest possible exposures to see if a feature corresponding to the 1.3-eV peak can be found, i.e., a peak corresponding to the very initial stages of chemisorption on Al(100) before island formation occurs.

We have calculated the values of the Al $2p$ orbital eigenvalues for the $\text{Al}_{25} + \text{O}$ cluster and the results are presented in Table II. For $Z_0 = 2.0$ the largest effect of the oxygen is as expected for the four aluminum atoms labeled 1 in Fig. 2 and we calculate a shift of 0.65 eV with respect to the clean aluminum value. When the oxygen is in the surface layer the $2p$ levels for Al(1) are shifted by 1.05 eV and the aluminum atom directly below the oxygen has its $2p$ levels shifted by 1.21 eV, quite close to the value found for the chemisorptive state on Al(111). It has already been suggested that the close-packed (111) surface reconstructs on oxygen incorporation and the close agreement between the $2p$ shifts calculated for low coverage on Al(100) and the observed shift on Al(111) might indicate that the local region about the oxygen atom on reconstructed (111) is similar to an unreconstructed (100) surface. The low value of the shift for $Z_0 = 2.0$ is further evidence that this is not the actual position of the oxygen atoms.

IV. CONCLUSIONS

The calculations described above have served two general purposes. First, information on the initial stages of the oxidation of aluminum has

been obtained. Our most extensive model, $Al_{25}+O$, gives a reasonable account of the most prominent features of the photoemission spectra and at the same time suggests the presence of further oxygen related structure which has not yet been conclusively identified in the experiments. This point is currently under further investigation experimentally³⁵ and thus a useful interplay between theory and experiment has been established. The calculations have also added further evidence, by examining the positions of the valence and core photoemission peaks as a function of the oxygen position, for the incorporation of oxygen into the surface even at low exposure. In general adatom positions are very difficult to determine both experimentally and theoretically (i.e., by total energy calculations) and we believe that the present procedure of examining the geometry dependence of a property other than the total energy and thereby obtaining geometrical information in an indirect manner will prove useful in the future for other systems. Finally, examination of the wave functions has provided information on the nature of the binding in the Al+O system; bonding and nonbonding orbitals were identified and correlated with features in the density of states.

The second general purpose of the calculations was to examine the requirements for a valid physical and computational cluster model for a rather

stringent test case, namely that of an approximately free-electron-like metal. This involved calculations for a series of clusters of increasing size. For the present case, it was found that up to third neighbors of the adsorbate were necessary ($Al_{25}+O$). The smaller clusters examined were inadequate. Similar convergence studies should be performed for other systems. We also found for this system that it is vital to achieve self-consistency; non-self-consistent calculations give qualitatively different results. To summarize, we conclude that the SCF- $X\alpha$ -SW cluster method is capable of providing quantitatively useful results on chemisorption if a sufficient number of atoms are included in the substrate cluster. Fortunately, it appears that the required number is small enough that the calculations are feasible.

Future work on the Al+O system will involve investigations of other crystal faces for which photoemission results are now being obtained and calculations of the important photoemission intensity matrix elements.

ACKNOWLEDGMENTS

This work was started while one of us (D.R.S.) was at the General Electric Co. and their support during that period is gratefully acknowledged, as is financial support from the National Research Council of Canada and l'Université de Montréal.

¹D. R. Salahub and R. P. Messmer, Phys. Rev. B (to be published).

²R. P. Messmer and D. R. Salahub, Int. J. Quantum Chem. **10S**, 183 (1976).

³R. P. Messmer and D. R. Salahub, in *Computers in Chemical Research and Education*, edited by E. V. Ludeña, N. Sabelli and A. C. Wahl (Plenum, New York, 1977), p. 156.

⁴R. P. Messmer and D. R. Salahub, Chem. Phys. Lett. **49**, 59 (1977).

⁵For example, F. A. Cotton and G. Wilkinson, *Advanced Inorganic Chemistry*, 3rd ed. (Wiley-Interscience, New York, 1972), p. 262.

⁶E. E. Huber, Jr. and C. T. Kirk, Jr., Surf. Sci. **5**, 447 (1966).

⁷G. Dorey, Surf. Sci. **27**, 311 (1971).

⁸W. H. Krueger and S. R. Pollack, Surf. Sci. **30**, 263 (1972).

⁹P. O. Gartland, Surf. Sci. **62**, 183 (1977), and references cited therein.

¹⁰R. J. Baird and C. S. Fadley, in Proceedings of the International Study Conference on Photoemission from Surfaces Noordwijk, Holland, September 13-16, 1976 (unpublished).

¹¹P. H. Dawson, Surf. Sci. **57**, 229 (1976).

¹²S. A. Flodström, L.-G. Petersson, and S. B. M. Hag-

ström, J. Vac. Sci. Technol. **13**, 280 (1976).

¹³K. Y. Yu, J. N. Miller, P. Chye, W. E. Spicer, N. D. Lang, and A. R. Williams, Phys. Rev. B **14**, 1446 (1976).

¹⁴S. A. Flodström, L.-G. Petersson, and S. B. M. Hagström, Solid State Commun. **19**, 257 (1976).

¹⁵S. A. Flodström, R. Z. Bachrach, R. S. Bauer, and S. B. M. Hagström, Phys. Rev. Lett. **37**, 1282 (1976).

¹⁶C. Martinsson, L.-G. Petersson, S. A. Flodström, and S. B. M. Hagström, in Ref. 10.

¹⁷N. D. Lang and A. R. Williams, Phys. Rev. Lett. **34**, 531 (1975).

¹⁸J. Harris and G. S. Painter, Phys. Rev. Lett. **36**, 151 (1976).

¹⁹See, e.g., D. R. Salahub, R. P. Messmer, and K. H. Johnson, Mol. Phys. **31**, 529 (1976), and references cited therein.

²⁰For recent reviews, see e.g., K. H. Johnson, Ann. Rev. Phys. Chem. **26**, 39 (1975); R. P. Messmer, in *Modern Theoretical Chemistry*, edited by G. A. Segal (Plenum, New York, 1977), Vol. 8, p. 215; N. Röscher, in *Electrons in Finite and Infinite Structures*, edited by P. Phariseau (Plenum, New York, to be published).

²¹R. P. Messmer, in *The Nature of the Surface Chemical Bond*, edited by G. Ertl and T. N. Rhodin (North-

- Holland, Amsterdam, to be published).
- ²²D. R. Salahub, A. E. Foti, and V. H. Smith, Jr. (unpublished).
- ²³B. Feuerbacher and R. F. Willis, *Phys. Rev. Lett.* 36, 1339 (1976).
- ²⁴R. J. Smith, J. Anderson, J. Hermanson, and G. J. Lapeyre, *Solid State Commun.* 21, 459 (1977).
- ²⁵C. L. Allyn, T. Gustafsson, and E. W. Plummer, *Chem. Phys. Lett.* 47, 127 (1977).
- ²⁶J. W. Davenport, *Phys. Rev. Lett.* 36, 945 (1976).
- ²⁷J. C. Slater, in *Advances in Quantum Chemistry*, edited by P. O. Löwdin (Academic, New York, 1972), Vol. 6, p. 1, and references cited therein.
- ²⁸K. H. Johnson, in Ref. 27, Vol. 7, p. 143, and references cited therein.
- ²⁹F. Herman, A. R. Williams, and K. H. Johnson, *J. Chem. Phys.* 61, 3508 (1974).
- ³⁰J. G. Norman, Jr., *J. Chem. Phys.* 61, 4630 (1974).
- ³¹K. H. Schwarz, *Phys. Rev. B* 5, 2466 (1972).
- ³²J. A. Tossell, *J. Am. Chem. Soc.* 97, 4840 (1975).
- ³³J. A. Tossell, *J. Phys. Chem. Solids* 36, 1273 (1975).
- ³⁴S. Evans, *J. Chem. Soc. Faraday II*, 1044 (1975).
- ³⁵S. B. M. Hagström (private communications).